1-1-1973

Experimental investigation of a cascaded system of vortex tubes

Robert Harlan Lubbers
Iowa State University

Experimental investigation of a cascaded system of vortex tubes

by

Robert Harlan Lubbers

A Thesis Submitted to the
Graduate Faculty in Partial Fulfillment of
The Requirements for the Degree of
MASTER OF SCIENCE

Department: Chemical Engineering
and Nuclear Engineering
Major: Nuclear Engineering

Iowa State University
Ames, Iowa

1973

TABLE OF CONTENTS

INTRODUCTION

The vortex tube -- or Ranque-Hilsch vortex tube, as it is sometimes called -- is a device capable of splitting a stream of compressed air into two streams of differing temperatures. Temperature differences of 250°C between the hot and the cold stream have been reported, and it has been suggested that the vortex tube might be employed in the production of liquid air.

The first vortex tube was designed by M. G. Ranque in 1932 and since that time it has been of interest to experimenters and theoreticians alike. The experimenters, on the whole have been the more successful -- the complex equations governing the flow in the vortex tube have made difficult an exact solution by direct application of theory. Although several authors have obtained analytical equations governing the temperature of the cold outlet (This, rather than the hot outlet, has been of interest to researchers.), these equations do not provide a particularly accurate reflection of experimental data or other analytical solutions.

Several factors are in agreement in the analytical and experimental results, however. Of particular interest to this author is the fact that the temperatures of the outlets tend to follow the input temperatures. That is to say, as the input gas is made cooler, the hot and cold output temperatures are decreased accordingly. This fact leads to the possibility of a cascaded system of vortex tubes -- a system in which the

hot exhaust of a primary tube is used to feed a secondary tube which produces its hot exhaust at an appropriately elevated temperature; likewise, the cold exhaust temperature of another secondary vortex tube would be depressed.

The vortex tube has several practical applications, none of which, however, have attempted to make use of both the hot and the cold streams of air exhausted. In cases where only the cold stream was employed, the efficiency was found to be comparable to ordinary refrigeration techniques. However, if a process requires, at different points, both heating and cooling, an economic advantage may be attained. This author's purpose is to investigate the characteristics of a cascaded system of vortex tubes and it's applicability to a modeling study, in order to provide a basis for further studies in application or economic feasibility. This paper will concern itself with both the heating and the cooling effects of the vortex tube, in the event that either, or both, may be pertinent to future applications.

SUMMARY OF PREVIOUS WORK

The operation of the vortex tube was first studied by M. G. Ranque and was described in a paper published by him in 1933. He received a French patent on his tube in 1932 and an American patent a year later. His paper and patents failed to arouse the interest of his fellow engineers and scientists until World War II when its first application was seen as a refrigerating device for the experimental German rocket plane. Ranque's tube was studied in greater detail by a German, R. Hilsch, whose research was outlined in an article published in 1947 (3). In this publication, Hilsch gave the temperature separating tube a name -- "Wirbelröhre" -- whose liberal English translation is "Vortex Tube." The report included optimization studies relating to the geometry of the tube, a tabulation of what Hilsch found to be the variables upon which the outlet gas temperatures were dependent, and detailed data of the variation of output temperatures with respect to μ (the ratio of the cold air mass flow rate to the mass flow rate of the input air). Hilsch was impressed with the temperature separations achieved. Describing it as "astonishing", he said: "With proper choice of μ and $1-\mu$, compressed air of a few atmospheres pressure and 20°C will easily produce a temperature of 200°C at the left [hot] tube and -50°C in the right [cold] tube." (3).

SUMMARY OF PREVIOUS WORK

The operation of the vortex tube was first studied by M. G. Ranque and was described in a paper published by him in 1933. He received a French patent on his tube in 1932 and an American patent a year later. His paper and patents failed to arouse the interest of his fellow engineers and scientists until World War II when its first application was seen as a refrigerating device for the experimental German rocket plane. Ranque's tube was studied in greater detail by a German, R. Hilsch, whose research was outlined in an article published in 1947 (3). In this publication, Hilsch gave the temperature separating tube a name -- "Wirbelröhre" -- whose liberal English translation is "Vortex Tube." The report included optimization studies relating to the geometry of the tube, a tabulation of what Hilsch found to be the variables upon which the outlet gas temperatures were dependent, and detailed data of the variation of output temperatures with respect to μ (the ratio of the cold air mass flow rate to the mass flow rate of the input air). Hilsch was impressed with the temperature separations achieved. Describing it as "astonishing", he said: "With proper choice of μ and 1-μ, compressed air of a few atmospheres pressure and 20°C will easily produce a temperature of 200°C at the left [hot] tube and -50°C in the right [cold] tube." (3).

Several applications have been found for the vortex tube, in addition to its employment in the German rocket planes during World War II. The New York Central Railroad found that the vortex tube could be used economically (due to the accessibility of compressed air) to cool drinking water on its passenger trains. According to Vivian (14), the unit, called the Vortacool, operates at 140 psig. and temperatures as low as -20°F have been reported. The Vortacool maintains water in a two-gallon tank at 50°F by means of an on-off thermostatic control. Vortex tubes have also been used in personal "air conditioning" units for use in hot environments by fire fighters, etc. These units are powered by tanks of compressed air; the cold flow of vortex tube piped through small tubes in the protective clothing of the user. After his investigation, Merkulov (6) predicted that the vortex tube could be used as a simple laboratory device for the production of liquid air.

Much of the literature concerning the vortex tube deals with optimization studies. These studies, based for the most part on experimentation, were explored most intensely by Martynovskii and Alekseev (5) whose method involved the use of a set of interchangeable vortex chambers, in which certain parameters were varied independently. Their work delved into the effects of inlet nozzle position and size, length of the hot tube, size and shape of the cold orifice, and shape of the cold diaphragm. Some of the conclusions reported by

Figure 1. Photograph of vortex tube with detail of vortex chamber

Martynovskii and Alekeev were

1. The best temperature separation, at a given tube diameter, is achieved when two tangential inlet nozzles are employed. (Vortex chambers with 1, 2, and 4 inlets were compared.)
2. The optimum cold orifice is circular and concentric with the axis of the vortex. It was noted, however, that some cooling effect was measured even with orifices of maximum eccentricity.
3. The best cold diaphragm is planar, with a surface perpendicular to the axis of the tube.
4. The optimum ratio of the radius of the vortex tube to the radius of the cold orifice is approximately 2.0.
5. The diameter of the vortex chamber is equal to the diameter of the cylindrical hot tube for most efficient cooling.
6. A variation of the input air temperature over a range of 7°C to 25°C resulted in no measurable effect on the output temperature differences.
7. The thermal separation effect of increasingly larger tubes also increased. (As diameter increased, so did the maximum temperature drop for a constant input pressure.)

The reported optima have not been verified analytically. Items numbered 2 and 4 are consistent with the theory as expressed by Lay (4). His temperature profile shows that the

Martynovskii and Alekseev were

1. The best temperature separation, at a given tube diameter, is achieved when two tangential inlet nozzles are employed. (Vortex chambers with 1, 2, and 4 inlets were compared.)

2. The optimum cold orifice is circular and concentric with the axis of the vortex. It was noted, however, that some cooling effect was measured even with orifices of maximum eccentricity.

3. The best cold diaphragm is planar, with a surface perpendicular to the axis of the tube.

4. The optimum ratio of the radius of the vortex tube to the radius of the cold orifice is approximately 2.0.

5. The diameter of the vortex chamber is equal to the diameter of the cylindrical hot tube for most efficient cooling.

6. A variation of the input air temperature over a range of 7°C to 25°C resulted in no measurable effect on the output temperature differences.

7. The thermal separation effect of increasingly larger tubes also increased. (As diameter increased, so did the maximum temperature drop for a constant input pressure.)

The reported optima have not been verified analytically. Items numbered 2 and 4 are consistent with the theory as expressed by Lay (4). His temperature profile shows that the temperature decreases as the axis of the vortex is approached. According to Martynovskii and Alekseev, as the cold orifice radius is decreased, the colder, central region is drawn out of the core. A smaller orifice, however, results in a smaller mass flow rate of cold air. A question arises as to the cooling effectiveness of the cold stream: is a small amount of cold air or a greater mass flow of warmer air the more effective? Martynovskii and Alekseev chose to place the optimum at the point where the cold orifice is one-half the diameter of the vortex tube.

Item 6 was refuted theoretically by Solokov (12) and experimentally by Brodyanskii and Martynov (1) and Merkulov (6). Solokov's analysis shows that $(T_n-T_c)/T_n$ is the factor which remains constant (rather that T_n-T_c) when input pressures and μ are fixed and the input temperature varies. (T_n is the input air temperature, T_c and T_h are the temperatures of the cold and the hot streams, respectively.) Brodyanskii and Martynov noted that as input temperature increased, so did ΔT_c ($=T_n-T_c$) and ΔT_h ($=T_h-T_n$). They observed no direct proportionality between the temperature separation effect and the input air temperature, however. Merkulov noted only that as T_n increased, so did ΔT_c.

Hilsch (3) agreed with item 7 and reported another optimum condition -- that the ratio of the tube diameter to the inlet nozzle diameter be approximately four. Sibulkin (10) considered rectangular inlet nozzles and concluded that the height of the inlet (its dimension along a radius of the vortex chamber) was the most significant dimension involved, with respect to the temperature separation.

An interesting effect was noted by Cooney (2). In a classroom demonstration of the vortex effect, he noticed a sizable instantaneous decrease in the temperature of the cold stream upon shut-off of the air supply.

The flow characteristics were analyzed in detail by Lay (4). He, as well as other theoreticians, based his analysis on the assumption of a quasi-solid vortex in the central region (the "cold core"). Around this free vortex the flow is directed axially. This assumption is verified experimentally and is shown in Figure 2.

Sibulkin (10), by assuming a perfect gas and a Mach number much less than one, analytically confirmed the axial

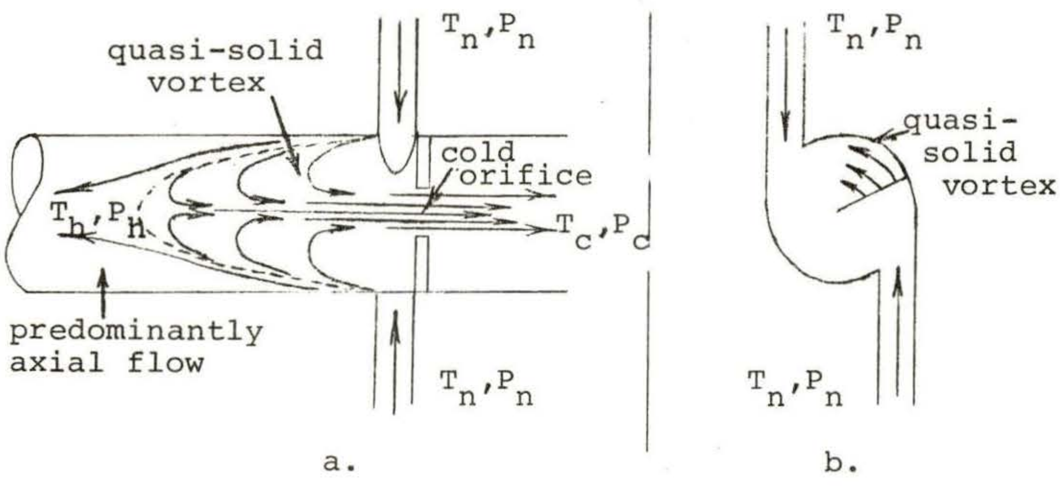

Figure 2. Flow pattern in a vortex tube

considered rectangular inlet nozzles and concluded that the height of the inlet (its dimension along a radius of the vortex chamber) was the most significant dimension involved, with respect to the temperature separation.

An interesting effect was noted by Cooney (2). In a classroom demonstration of the vortex effect, he noticed a sizable instantaneous decrease in the temperature of the cold stream upon shut-off of the air supply.

The flow characteristics were analyzed in detail by Lay (4). He, as well as other theoreticians, based his analysis on the assumption of a quasi-solid vortex in the central region (the "cold core"). Around this free vortex the flow is directed axially. This assumption is verified experimentally and is shown in Figure 2.

Sibulkin (10), by assuming a perfect gas and a Mach number much less than one, analytically confirmed the axial

Figure 2. Flow pattern in a vortex tube

flow pattern shown in Figure 2a. Figure 3 may be compared to Figure 2a -- it describes the axial flow in a plane containing the inlet orifice and the center line.

The temperature separation arises, according to Smith (11) and others, from three effects.

1. Heat transfer as a result of a temperature gradient -- conduction.

2. Heat transfer as a result of a pressure gradient -- convection.

3. Shear forces within the fluid and by the fluid against the tube wall.

The third effect is of questionable significance according to Martynovskii and Alekseev (5). One of their vortex tubes employed a moveable inner wall which was allowed to rotate at

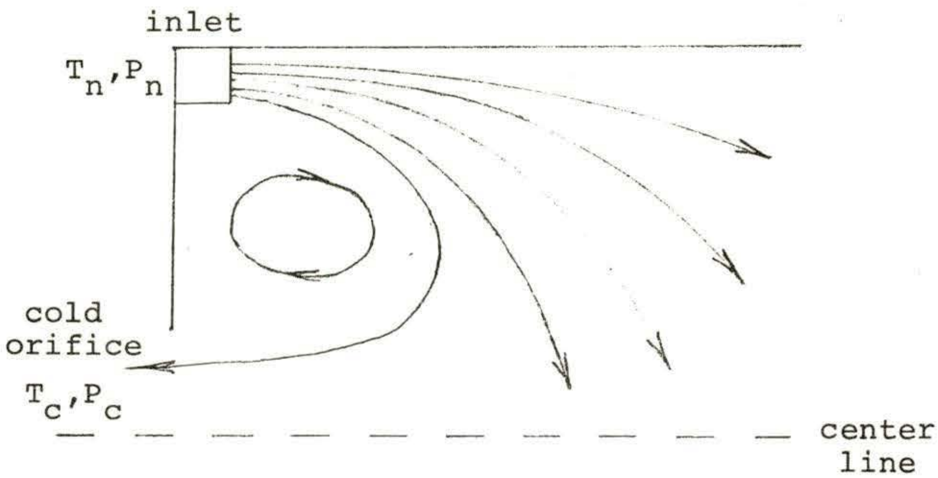

Figure 3. Axial flow pattern

the velocity of the fluid near its surface. No measurable difference in temperature separation was found.

Work by Merkulov and Kolyshev (7) indicated that the second effect, that of the pressure gradient, was predominant. Their paper was not available, but an abstract found in Applied Mechanical Reviews states: "It was demonstrated experimentally that the principal influence on the cooling effect in the vortex tube proved to be the extent of the expansion of the vortex, the influence of the other parameters being insignificant."

One of the most thorough and applicable analyses is that carried out by Solokov (12). He not only derived a formula for the temperature drop to the cold end as a function of input temperature, parameters dependent upon the pressure ratio (input pressure/ pressure of the cold stream), and the mass flow rate μ; he also solved the derived equation for a given set of input conditions. According to Solokov, the thermal separation effect may be described by the T-S diagram in Figure 4. Table 1 is an explanation of the processes involved.

In the analysis of the cold stream, the differential throttle effect ($\partial T/\partial P$) is assumed to be negligible between points 3 and 4. Therefore $T_c = T_c{}'$, the stagnation temperature. The cold exhaust temperature is

$$T_c = \frac{V^2}{2c_p} + T_2 = \frac{(\bar{w}_t{}^2 + \bar{w}_o{}^2)}{2c_p} + T_2 , \qquad (1)$$

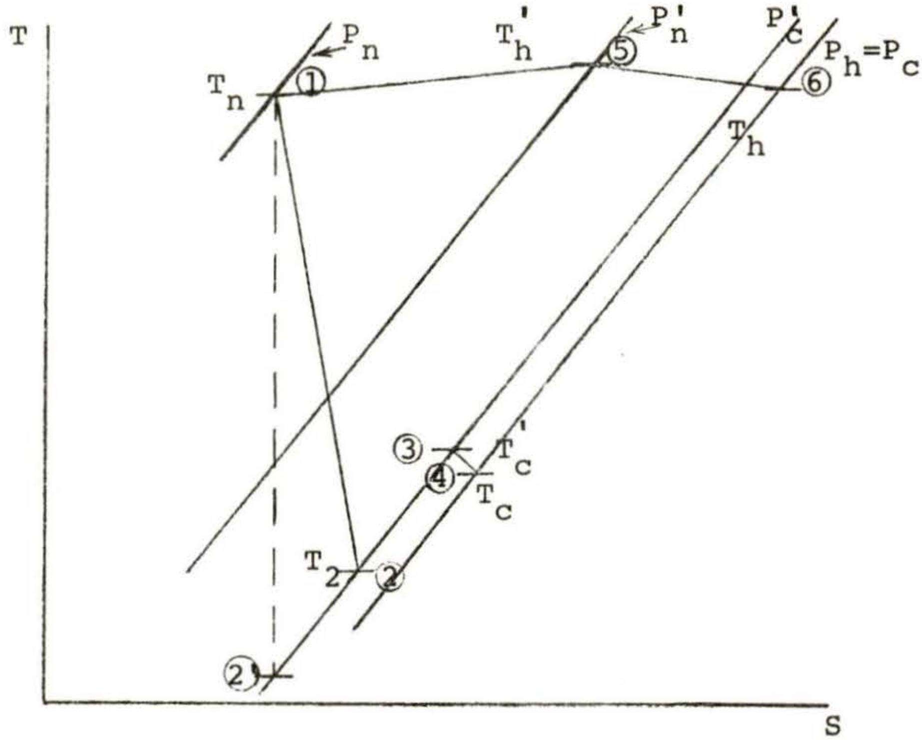

Figure 4. T-S diagram of vortex tube operation

Table 1. Explanation of processes involved in Figure 4

Temperature change		Process
1	2'	Ideal expansion from input pressure to pressure at orifice.
1	2	Real expansion. ($\Delta S>0$ due to irreversibility.)
2	3	Stagnation temperature of gas at orifice plate: $T_c'=T_2 + (V^2/2c_p)$.
3	4	Expansion from P_c' at orifice to P_c beyond orifice.
1	5	Compression from input pressure to pressure in hot tube.
5	6	Expansion from P_h' in hot tube to P_h upon exhaust.

where $\bar{w}_t$ is the average tangential velocity and $\bar{w}_o$ is the average axial velocity. T_c is desired as a function of more easily measured variables (namely pressures and flow rates), so the unknowns $\bar{w}_t^{\,2}$, $\bar{w}_o^{\,2}$, and T_2 must be expressed in these terms.

T_2 may be shown to be

$$T_2 = T_n - \phi^2 \frac{\lambda^2 a_n^{*2}}{2c_p}$$

where a_n^* is the critical velocity of the input stream, λ^2 is the corrected adiabatic velocity factor (velocity during adiabatic expansion/a_n^*), and ϕ is an empirical factor which is determined experimentally to be approximately 0.75. Since

$$a_n^* = \sqrt{\frac{k-1}{k+1}\, 2c_p T_n}$$

$$T_2 = T_n \left[1 - \left(\frac{k-1}{k+1}\right)\phi^2 \lambda^2\right] \qquad (2)$$

In Equation 2, $k = c_p/c_v$, ϕ is known, and λ may be determined from P_c/P_n -- the pressure just beyond the cold orifice/the inlet pressure.

The tangential velocity, w_t, at given distance from the center of the quasi-solid vortex, is, for a tube of radius r_t

$$w_t(r) = \lambda a_n^* \frac{r}{r_t} \, .$$

where $\bar{w}_t$ is the average tangential velocity and $\bar{w}_o$ is the average axial velocity. T_c is desired as a function of more easily measured variables (namely pressures and flow rates), so the unknowns $\bar{w}_t^{\,2}$, $\bar{w}_o^{\,2}$, and T_2 must be expressed in these terms.

T_2 may be shown to be

$$T_2 = T_n - \beta^2 \frac{\lambda^2 a_n^{*2}}{2c_p}$$

where a_n^* is the critical velocity of the input stream, λ^2 is the corrected adiabatic velocity factor (velocity during adiabatic expansion$/a_n^*$), and β is an empirical factor which is determined experimentally to be approximately 0.75. Since

$$a_n^* = \sqrt{\frac{k-1}{k+1}\, 2c_p T_n}$$

$$T_2 = T_n\left[1-\left(\frac{k-1}{k+1}\right)\beta^2\lambda^2\right] \qquad (2)$$

In Equation 2, $k=c_p/c_v$, β is known, and λ may be determined from P_c/P_n -- the pressure just beyond the cold orifice/the inlet pressure.

The tangential velocity, w_t, at given distance from the center of the quasi-solid vortex, is, for a tube of radius r_t

$$w_t(r) = \lambda a_n^* \frac{r}{r_t}.$$

The average tangential velocity in the region determined by the orifice diameter is shown to be

$$\bar{w}_t = \frac{1}{f_c} \int_o^{r_c} \lambda a_n{}^* \frac{r}{r_t}(2\pi r)\, dr = 0.667\lambda a_n{}^* \frac{r_c}{r_t} . \qquad (3)$$

The cross sectional area of the cold stream (radius r_c) is f_c.

The average axial velocity, in terms of mass flow rates, G_c, of the cold stream, and G_n of the input stream is

$$\bar{w}_o = \frac{G_c}{f_c \rho_c} = \frac{\mu G_n v_c}{f_c} ,$$

where v_c is the specific volume of the air under the conditions of the cold stream. Introducing two new symbols -- $\varepsilon_n{}^*$ = density of the gas at critical velocity/density of the gas at stagnation conditions, and ε_c = density of the gas in the cold stream/density of the gas at stagnation conditions:

$$\bar{w}_o = \mu a_n{}^* \frac{f_n}{f_c} \frac{\varepsilon_n{}^*}{\varepsilon_c} \qquad (4)$$

(f_n is the cross-sectional area of the inlet nozzle.) By combining Equations 1, 2, 3, and 4, and defining $\varepsilon_c \lambda / \varepsilon_n{}^*$ as q_c, which is the ratio of the axial mass velocity of the adiabatically moving cold stream to the mass velocity of the flow in a critical section, an equation for the temperature drop to the cold stream may be derived as

The average tangential velocity in the region determined by the orifice diameter is shown to be

$$\bar{w}_t = \frac{1}{f_c}\int_0^{r_c} \lambda a_n{}^* \frac{r}{r_t}(2\pi r)\,dr = 0.667\lambda a_n{}^* \frac{r_c}{r_t}\,. \qquad (3)$$

The cross sectional area of the cold stream (radius r_c) is f_c.

The average axial velocity, in terms of mass flow rates, G_c, of the cold stream, and G_n of the input stream is

$$\bar{w}_c = \frac{G_c}{f_c \rho_c} = \frac{\mu G_n v_c}{f_c}\,,$$

where v_c is the specific volume of the air under the conditions of the cold stream. Introducing two new symbols -- $\varepsilon_n{}^*$ = density of the gas at critical velocity/density of the gas at stagnation conditions, and ε_c = density of the gas in the cold stream/density of the gas at stagnation conditions:

$$\bar{w}_c = \mu a_n{}^* \frac{f_n}{f_c}\frac{\varepsilon_n{}^*}{\varepsilon_c} \qquad (4)$$

(f_n is the cross-sectional area of the inlet nozzle.) By combining Equations 1, 2, 3, and 4, and defining $\varepsilon_c\lambda/\varepsilon_n{}^*$ as q_c, which is the ratio of the axial mass velocity of the adiabatically moving cold stream to the mass velocity of the flow in a critical section, an equation for the temperature drop to the cold stream may be derived as

$$\frac{\Delta T_c}{T_n} = \frac{k-1}{k+1} \lambda^2 \left[\phi^2 - 0.445 \frac{f_c}{f_t} - \frac{\mu^2}{q_d^{\,2}} \frac{f_n^{\,2}}{f_c^{\,2}} \right]$$

A heat balance may be used to show that if the specific heat remains constant $\Delta T_h = \Delta T_c \mu/(1-\mu)$. The temperature rise in the hot tube is accordingly related to the temperature drop.

$$\frac{\Delta T_h}{T_n} = \frac{\mu}{1-\mu} \frac{k-1}{k+1} \lambda^2 \left[\phi^2 - 0.445 \frac{f_c}{f_t} - \frac{\mu^2}{q_d^{\,2}} \frac{f_n^{\,2}}{f_c^{\,2}} \right]$$

In the previous work surveyed, the possibility of obtaining either higher or lower temperatures by utilizing the hot and cold outputs of one vortex tube as inputs to secondary tubes was not investigated. By this cascaded system, it is conjectured that lower (as well as higher) temperatures might be obtained for a given pressure of available compressed air. Before any application of this method can be attempted, however, the characteristics of the cooling effect must be studied and outlined. The compilation of these data is the purpose of this thesis.

SIGNIFICANT VARIABLES

The variables which may be significant in the analysis of the vortex thermal separation effect can be placed into three categories: those which specify the geometries of the vortex tubes, the dynamic variables of the tube, and the properties of the materials upon which the phenomenon depends.

The choice of geometric variables depends mostly on the available conditions for operation of the vortex tube. Limitations in the pressure gauges and flow meters used, as well as those imposed by the University compressed supply, restricted the size of the tubes used. In his study, which employed the same air supply as well as much of the same apparatus, Smith (11) found that a vortex chamber of about one inch diameter could be used successfully. Recommendations of other researchers (see Summary of Previous Work) were considered in determining the relative sizes of other components: The cold orifice was one-half the diameter of the vortex chamber, as suggested by Martynovskii and Aleksev (5). These authors also found that optimum temperature separation occurred for a tube length 15 - 20 times its diameter. Dual square inlets were used, whose cross-sectional dimension radial to the tube was approximately one-fourth the tube diameter, as suggested by Hilsch (3).

SIGNIFICANT VARIABLES

The variables which may be significant in the analysis of the vortex thermal separation effect can be placed into three categories: those which specify the geometries of the vortex tubes, the dynamic variables of the tube, and the properties of the materials upon which the phenomenon depends.

The choice of geometric variables depends mostly on the available conditions for operation of the vortex tube. Limitations in the pressure gauges and flow meters used, as well as those imposed by the University compressed supply, restricted the size of the tubes used. In his study, which employed the same air supply as well as much of the same apparatus, Smith (11) found that a vortex chamber of about one inch diameter could be used successfully. Recommendations of other researchers (see Summary of Previous Work) were considered in determining the relative sizes of other components: The cold orifice was one-half the diameter of the vortex chamber, as suggested by Martynovskii and Alekseev (5). These authors also found that optimum temperature separation occurred for a tube length 15 - 20 times its diameter. Dual square inlets were used, whose cross-sectional dimension radial to the tube was approximately one-fourth the tube diameter, as suggested by Hilsch (3).

The dynamic variables of interest include the temperatures, pressures, and mass flow rates. In this study, temperature differences were considered to be of primary importance, although the input temperature to each tube will be considered. Solokov's theory (12) will be employed to the extent of considering the ratio of temperature changes (ΔT_c and ΔT_h) to input temperature a constant, provided that only the input temperature varies. (This theory has been reinforced by preliminary observations.) The pressure ratio (input pressure over cold exit pressure, P_n/P_c or $\mathbb{P}$) will be considered as another of the dynamic variables. Support is gained here from Smith's dimensional analysis (11), from Solokov (12), and implied by Hilsch (3) and others. Finally, the cold-to-input mass flow rate ratio, μ, which is of common interest to all researchers, will be considered one of the dynamic variables.

The last group, the material properties of the gas and components of the tube, was studied in more detail by Smith (11) than in any of the other literature reviewed. Smith considered viscosity, thermal conductivities of the gas and of the tube material, and specific heats of the gas at constant pressure and volume. The viscosity, however, is not considered in analytical approaches of other authors since frictional forces are usually neglected among particles of the fluid. The effect of thermal conduction through the tube as well as through the gas is also neglected. (The thermal

The dynamic variables of interest include the temperatures, pressures, and mass flow rates. In this study, temperature differences were considered to be of primary importance, although the input temperature to each tube will be considered. Solokov's theory (12) will be employed to the extent of considering the ratio of temperature changes (ΔT_c and ΔT_h) to input temperature a constant, provided that only the input temperature varies. (This theory has been reinforced by preliminary observations.) The pressure ratio (input pressure over cold exit pressure, P_n/P_c or $\Re$) will be considered as another of the dynamic variables. Support is gained here from Smith's dimensional analysis (11), from Solokov (12), and implied by Hilsch (3) and others. Finally, the cold-to-input mass flow rate ratio, μ, which is of common interest to all researchers, will be considered one of the dynamic variables.

The last group, the material properties of the gas and components of the tube, was studied in more detail by Smith (11) than in any of the other literature reviewed. Smith considered viscosity, thermal conductivities of the gas and of the tube material, and specific heats of the gas at constant pressure and volume. The viscosity, however, is not considered in analytical approaches of other authors since frictional forces are usually neglected among particles of the fluid. The effect of thermal conduction through the tube as well as through the gas is also neglected. (The thermal conduction of the tube could be removed, essentially, by insulating the hot tube.) Ignoring the effects of viscous shear and conduction is in agreement with the findings, previously referred to, of Merkulov and Kolyshev (7) -- that the thermal separation in a vortex tube was due predominantly to the pressure gradient. The result, therefore, is that only the heat capacities, c_p and c_v, significantly affect the temperature separation. They appear in the ratio c_p/c_v, which is referred to as k. Solokov also includes a factor which is dependent upon the density of the gas, but states that the factor may be determined also from the pressure ratio, P_n/P_c. All significant variables are tabulated in Table 2.

The variables listed in Table 2 are collected, and it is assumed that

$$\Delta T_c = F(T_n, \lambda_i, d_c, P_n/P_c, Q_n, Q_c, c_p, c_v)$$

where λ_i is used to denote any length variable other than d_c. According to Buckingham's π-Theorem, there are six π-terms required; one of the many possible sets might be

$$\frac{\Delta T_c}{T_n} = F\left(\frac{\lambda_i}{d_c}, \frac{c_p}{c_v}, \frac{P_n}{P_c}, \frac{Q_c}{Q_n}, \frac{{Q_n}^2}{c_p T_n {d_c}^4}\right)$$

Each π-term is required to have equal values in both the model and the prototype.

Table 2. Significant variables

Variable	Definition
Geometric:	
d	Inside diameter of the tube
d_c	Diameter of the cold orifice
h,w	Cross-sectional dimensions of the inlet channel
ℓ	Length of the tube
Dynamic:	
ΔT_c	Temperature drop -- input to cold stream
ΔT_h	Temperature rise -- input to hot stream
T_n	Inlet temperature
P_n	Inlet pressure
P_c	Cold stream pressure
Q_n	Mass flow rate of inlet gas
Q_c	Mass flow rate of cold stream
Material:	
c_p	Specific heat (constant pressure)
c_v	Specific heat (constant volume)

This similitude treatment of the vortex tube results in equivalences of six π-terms. Of these equalities, two were found to be design conditions -- one implies the length scale (in this case 3/2) and the other is determined by material properties, being satisfied by using the same gas and construction material in both model and prototype.

The remaining equivalences define the operating conditions.

$$\frac{P_n}{P_c} = \frac{P_{nm}}{P_{cm}}$$

$$\frac{Q_c}{Q_n} = \frac{Q_{cm}}{Q_{nm}}$$

$$\frac{{Q_n}^2}{c_p T_n {d_c}^4} = \frac{{Q_{nm}}^2}{c_{pm} T_{nm} {d_{cm}}^4}$$

The subscript m denotes values in the model, and d_c is the diameter of the cold orifice. Smith (11) found that the third operating condition, which can be expressed as $Q_n/Q_{nm}=n^2$, was not satisfied exactly when the operating condition on the pressure ratios was satisfied. (n is the length scale.) He attributed this apparent redundancy to the fact that the length of the inlet channels was not scaled as the rest of the vortex tube. He allowed this operating condition to remain unfulfilled, and allowed the distortion to be absorbed in the prediction factor. Smith's prediction factor, however, was observed to be 1.0 $\pm$ 0.004, so that neglecting this discrepancy would appear justified.

The last of the π-terms results in his prediction equation.

$$\frac{\Delta T_c}{T_n} = \delta \frac{\Delta T_{cm}}{T_{nm}}$$

One more variable is included in the analysis -- ΔT_h. ΔT_h is, however, a function of ΔT_c, according to Solokov (12), and could be handled independently.

APPARATUS

The vortex tubes employed in this investigation were patterned after those used by Smith (11) in his similitude study of the vortex thermal separation effect. Smith's method of construction was followed for three reasons: this configuration resulted in prediction equation with a prediction factor of 1.0 $\pm$ 0.004, the interchangeability of the vortex tubes makes the system flexible enough for easy application to several cascading systems, and, finally, some of Smith's apparatus was still available for use. The vortex tubes in this study were fabricated of Plexiglas, since, at the pressures attained, these offered sufficient strength. Plexiglas was also advantageous because of its cost and easy workability.

Three configurations of cascading systems were studied. The first (referred to as system 1) consisted of three vortex tubes. The primary tube, in which the initial temperature separation occurs, is of a larger diameter than the two secondary tubes. One of the smaller tubes used the cold stream from the primary tube as its input. This tube was designated "secondary C." The other small tube, "secondary H," effects a temperature separation of the hot stream from the primary tube. The secondary tubes were smaller than the primary because it was believed that they would produce a more measurable temperature separation. (A smaller tube might be required since the flow rates into these tubes are less than the flow rate into the primary tube. By forcing this flow through a smaller tube, greater input pressures are attained, increasing $\mathbb{P}$, and the thermal separation is enhanced.) A schematic of system 1 is shown in Figure 5.

System 2 is similar to system 1 with the exception of the vortex tube secondary C, which was replaced with a tube of diameter equal to that of the primary tube. It was noted that in system 1, $\mathbb{P}^p$ (P_n^p/P_c^p for the primary tube[1]) could not be raised, via valve adjustments, high enough to obtain adequate temperature separations in the primary tube. The larger secondary C reduces the resistance to the flow through this tube, and therefore P_c^p. $\mathbb{P}^p$ is increased, as is the temperature separation. Figure 6 is a schematic diagram of system 2.

Finally, system 3 was devised to further reduce the cold stream pressure in the primary tube -- secondary C was removed altogether. It seemed conceivable that a greater cooling could be achieved by this increase in $\mathbb{P}^p$ than by cooling through another vortex tube. See Figure 7.

The systems studied were intended to consist of 3/4 inch and 1/2 inch tubes in the model and 1 1/8 inch and 3/4 inch tubes in the prototype. Plexiglas tubing of 1 1/8 inch inside diameter, however, was not available and one inch tubes were

---

[1]The superscript denotes which of the tubes is referred to: p for primary, c for secondary C, h for secondary H.

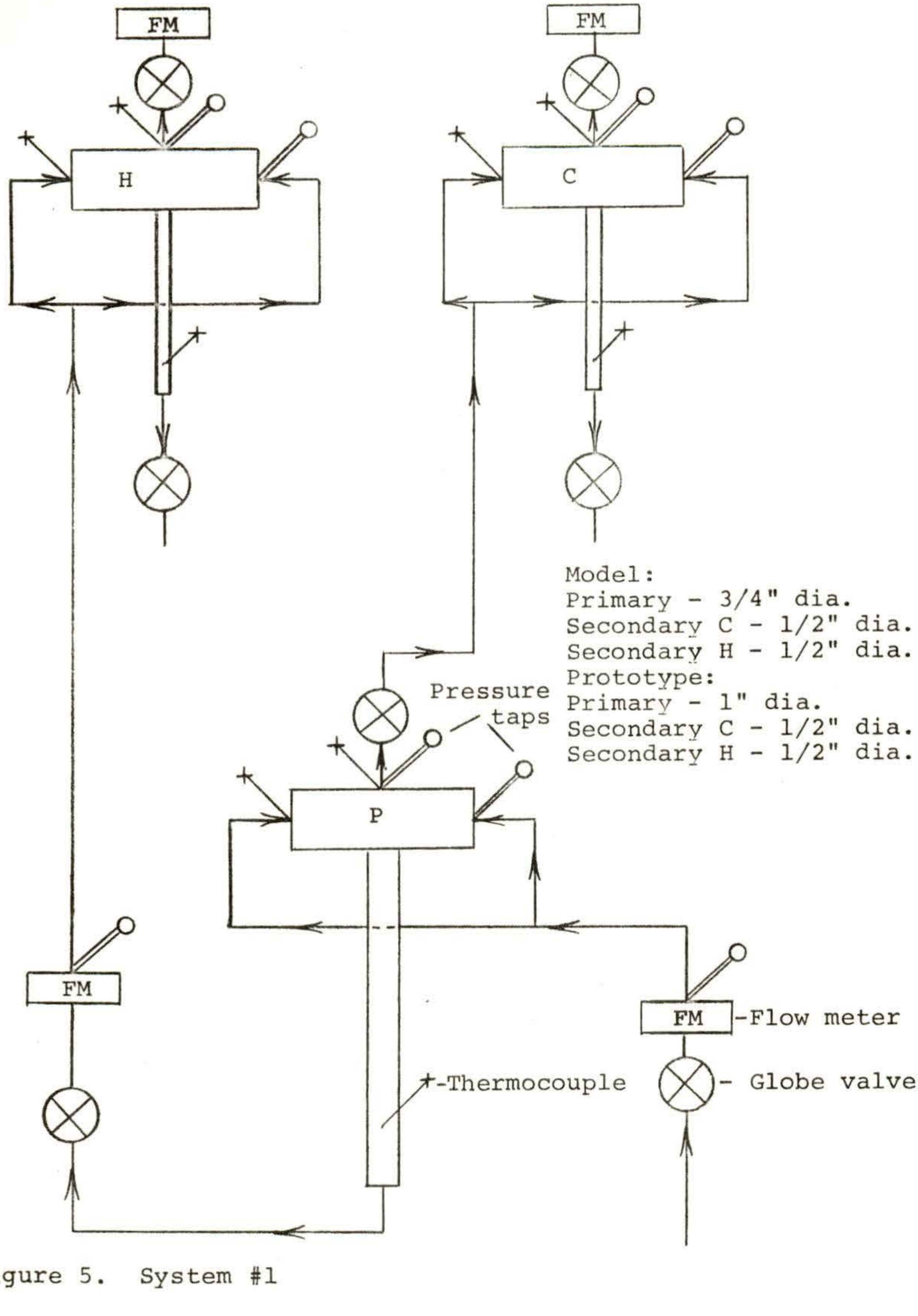

Figure 5. System #1

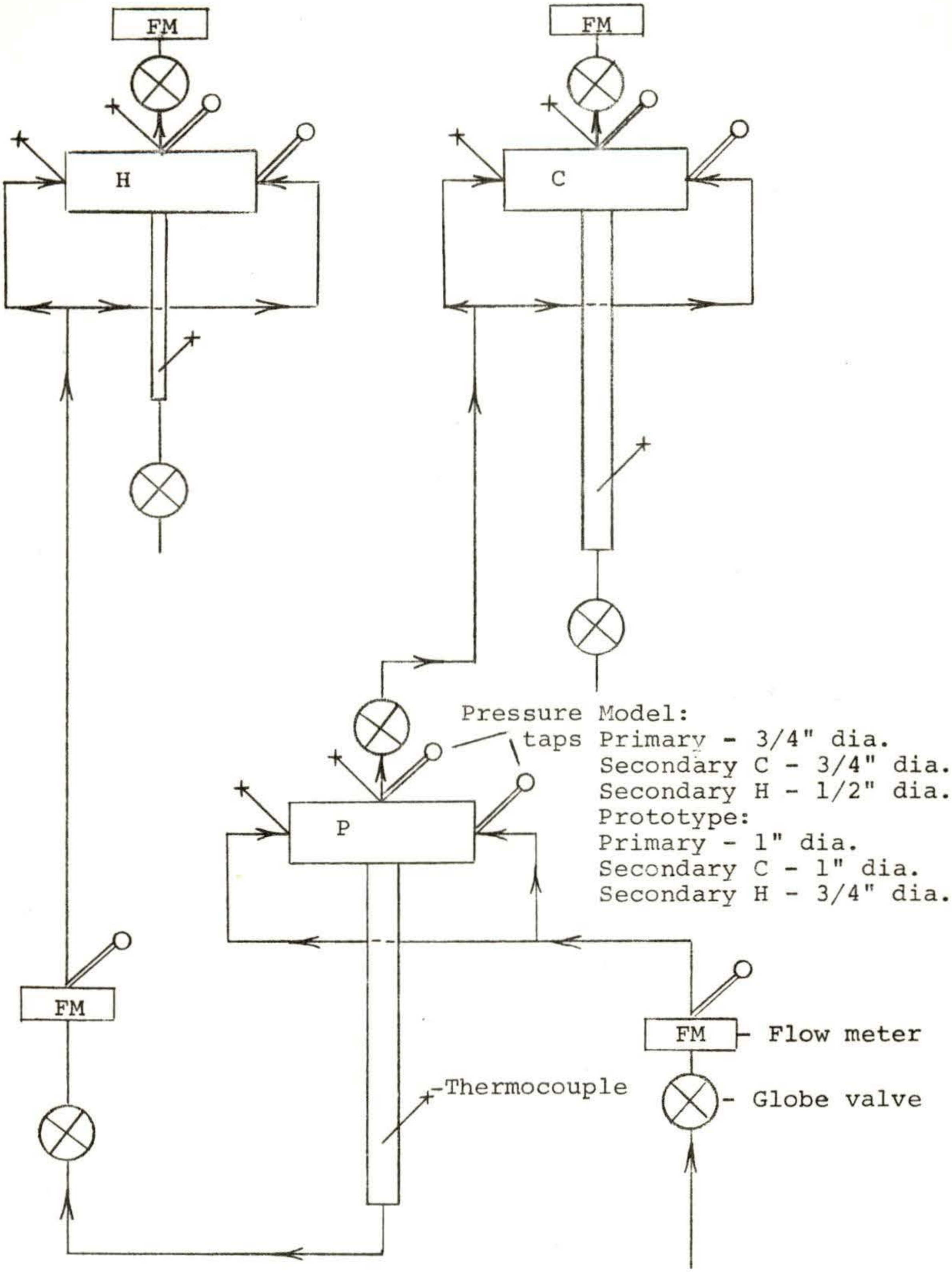

Figure 6. System #2

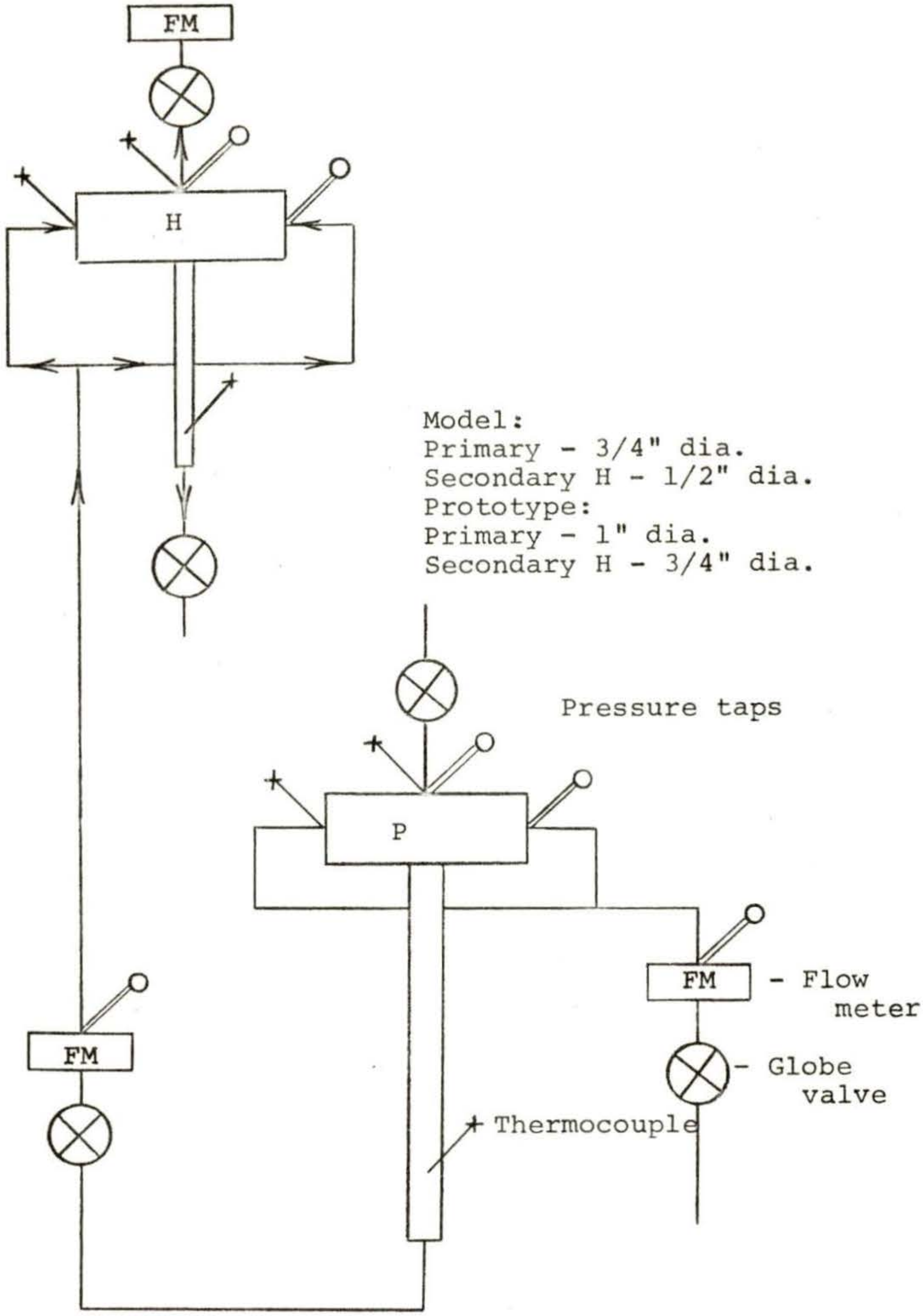

Figure 7. System #3

used instead. The effect of this small distortion in the modeling will be seen in the magnitudes of the flow rates. Smith (11) reports, though, that the operating condition requiring Q_n/Q_{nm} to equal n^2 may be in error by as much as 35% and still "be of no more than secondary significance." The other operating condition containing flow rates states that $\mu=\mu_m$ -- a condition which may still be met exactly by means of valve adjustments. For these reasons, it is expected that the use of a one inch tube in the prototype will not significantly affect the data.

EXPERIMENTAL PROCEDURE

The range over which data could be accumulated was found to be severely limited by the system. In a given configuration, the maximum value for the pressure ratio P_n/P_c was set by the impedance to the flow due to the secondary tubes. A minimum pressure ratio was encountered also, the limitation existing because of small temperature separation and instabilities in the flow meters and valves. In addition to this restriction on pressures, it was found that a full range of μ's was not attainable in several cases -- particularly in the primary tube. With these restrictions noted, data were obtained in whatever regions possible.

Problems were incurred in the stability of the air supply. The University compressed air, which was employed in this study, tended to vary in temperature from one reading to the next, as well as from day to day. Maintaining a constant input pressure was also found to be a problem. It was discovered, however, that this effect was less significant in the evenings. Whenever possible, therefore, data were accumulated after 5:00 P.M.

The pressure ratio in the primary tube was considered to be a constant parameter, and was set at the desired value by adjustments of the hot and cold exhaust valves of both secondary tubes. For example, as all four of these valves were closed, P_n/P_c in the primary tube decreased toward 1.0

EXPERIMENTAL PROCEDURE

The range over which data could be accumulated was found to be severely limited by the system. In a given configuration, the maximum value for the pressure ratio P_n/P_c was set by the impedance to the flow due to the secondary tubes. A minimum pressure ratio was encountered also, the limitation existing because of small temperature separation and instabilities in the flow meters and valves. In addition to this restriction on pressures, it was found that a full range of μ's was not attainable in several cases -- particularly in the primary tube. With these restrictions noted, data were obtained in whatever regions possible.

Problems were incurred in the stability of the air supply. The University compressed air, which was employed in this study, tended to vary in temperature from one reading to the next, as well as from day to day. Maintaining a constant input pressure was also found to be a problem. It was discovered, however, that this effect was less significant in the evenings. Whenever possible, therefore, data were accumulated after 5:00 P.M.

The pressure ratio in the primary tube was considered to be a constant parameter, and was set at the desired value by adjustments of the hot and cold exhaust valves of both secondary tubes. For example, as all four of these valves were closed, P_n/P_c in the primary tube decreased toward 1.0

and tended to increase as the valves were opened. With the pressure now a constant value, the flow rates through the primary tube were measured via the rotameters and the pressure correction factors employed to obtain the flow rate in SCFM at 70°F. (Correction factors for variation in temperatures were also available, but were of negligible effect.) With the values for P_n/P_c and μ now set, the appropriate temperatures were recorded. Both before and after the measurement of a temperature, all pressure gauges and flow meters were rechecked to assure that a change had not occurred. A short time after one set of temperatures was recorded (at least one minute) these temperatures were rechecked. If any temperature differed from its previous value by more than 0.2°F it was checked once again, after another short pause. When two successive sets of readings agreed in all details, that data was entered.

It was found that when all flow rates and pressure were set for the primary tube, the pressure ratios in the secondary tubes were constrained to a very small range. The flow rate fractions in the secondaries, however could be swept through nearly the full range of 0.0 to 1.0, while $\mathbb{P}$ for that secondary remained constant. Temperatures for the given conditions of $\mathbb{P}^p$, u^p, and $\mathbb{P}$ in the secondary tube could then be found as a function of μ in that secondary. The flow ratio was varied merely by opening one exhaust valve and closing the other. The same procedures involving double-checking of gauges and meters, and requirements of agreement between two successive readings were again followed in obtaining data points. In addition, while the μ value in the secondary was being varied, the temperatures of the input, hot stream and cold stream of the primary were also remeasured occasionally to note any change that had occurred in the cooling by the primary tube.

When a curve ($\Delta T/T_n$ versus μ) was obtained for one of the secondaries, the same procedure was followed in obtaining a similar curve for the other secondary. (Since it is presumed that secondary C will be used primarily to obtain cold air, only ΔT_c was measured. Likewise, ΔT_h was measured from secondary H. Both ΔT_c and ΔT_h were measured in the primary tube.) After curves were obtained for both secondary H and C, the exhaust valves for these tubes were readjusted, resulting in a new value of μ^p. $\mathbb{P}^p$ remaining constant, the entire process was repeated, resulting in new curves (at different $\mathbb{P}^h$ and $\mathbb{P}^c$) for the secondary tubes and a new data point for the primary tube.

When sufficient data of temperature ratios and μ had been tabulated for the primary tube, the pressure ratio in the primary was changed (if possible) and the previously described process was repeated. The final result is a family of curves (each at a different $\mathbb{P}$) showing the relationship of $\Delta T_c/T_n$ or $\Delta T_h/T_n$ as a function of μ for the primary tube and for each of the secondaries. Such a set of data was acquired for both the model and the prototype of each system.

In most cases, a pressure of 20 psig was employed at the input to the primary tube. It was found that this pressure resulted in flow rates which were measurable in the central region of the rotameters for both model and prototype. In a few instances, the input pressure was increased to 30 psig in an attempt to extend the range of attainable μ's.

RESULTS

As previously stated, the restriction on the attainable values of the pressure ratios, P_n/P_c, developed as the most binding of those encountered. It was found that in the model (3/4 inch primary tube) of system 1, the largest pressure ratio was 1.15. Smaller ratios could be reached, but these resulted in very small temperature separations. Data were unreliable at these lower pressure ratios due to instabilities in the flow meters and valves. System 2 was more versatile (as expected) and a $\mathbb{P}_m^p$ of 1.25 could be achieved as well as the previous value, 1.15. By using system 3, pressure ratios of 1.15, 1.25, and 1.35 could be reached. The same effect was seen in the prototype and data were gathered using the same primary pressure ratios. (One exception was the system 2 prototype -- a $\mathbb{P}$ of 1.25 could not quite be attained.)

The restriction governing the selection of $\mathbb{P}^p$'s was not an absolute inability to obtain a given value, but rather took the form of a decreasing range of μ's available to that $\mathbb{P}^p$. As the value of $\mathbb{P}^p$ increased above the upper value used, the range of μ's became so narrow as to make data inconclusive. Figures 10 and 12 display the reduction of the range of attainable μ's with increasing $\mathbb{P}^p$.

The results obtained showed that the parameters which produced the greatest effect on the output temperatures of the system were the pressure ratios of the secondary tubes. The

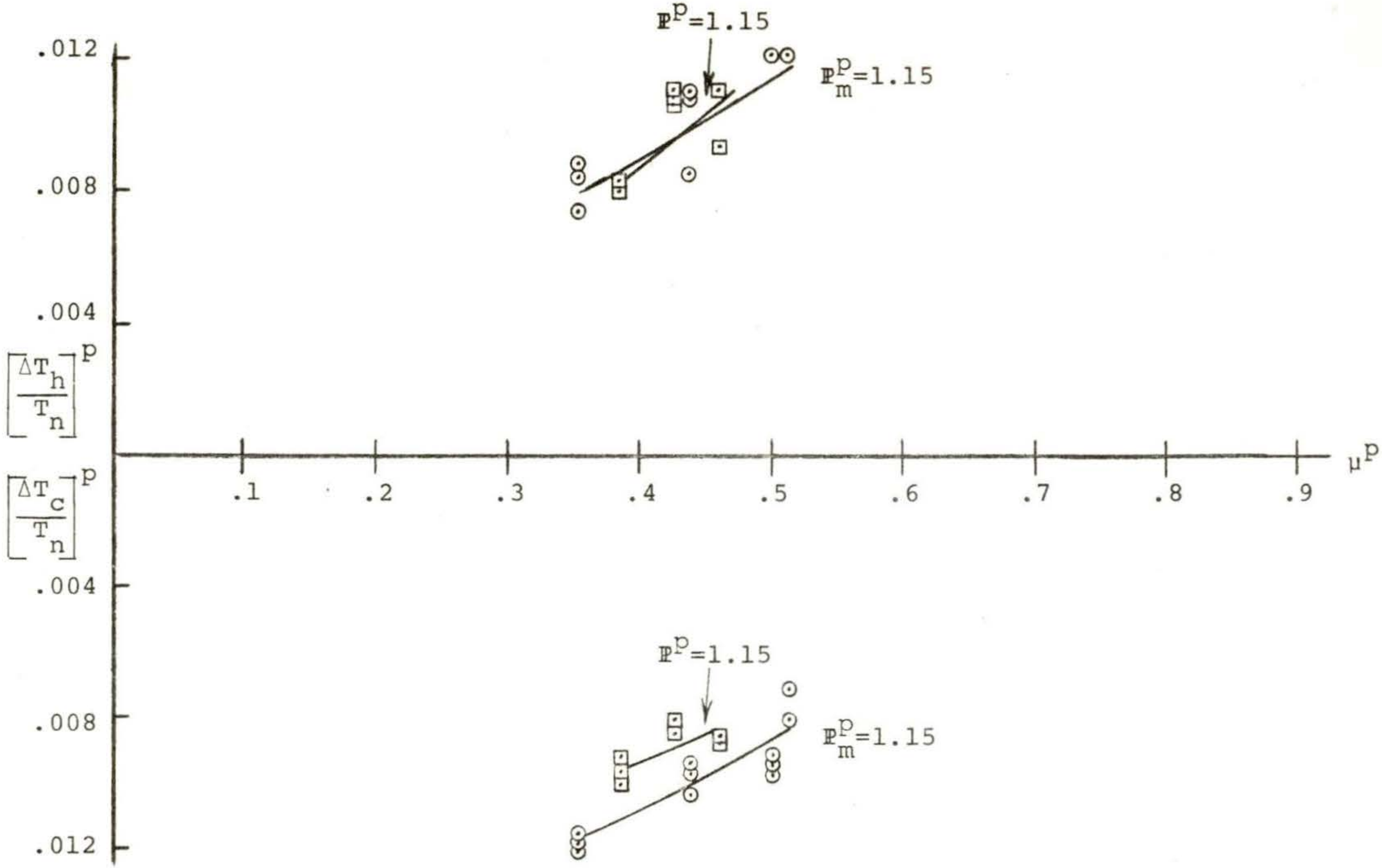

Figure 8. Temperature ratio versus flow ratio. Primary tube, system 1

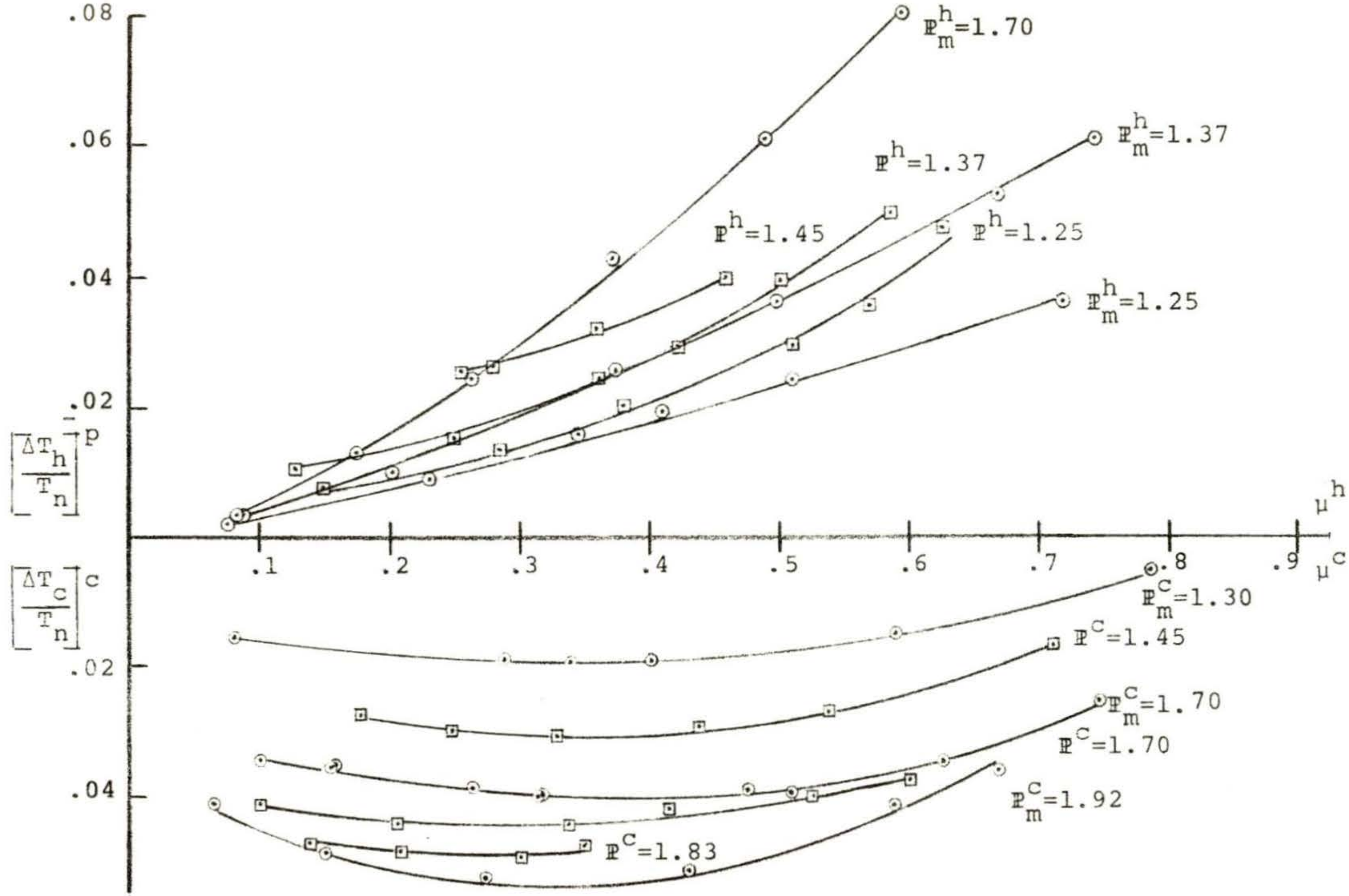

Figure 9. Temperature ratio versus flow ratio. Secondary H and secondary C, system 1

pressure ratio of the primary tube affects the temperature in the same manner, but in the systems studied, its magnitude was severely limited.

The data are presented in the form of graphs of $\Delta T/T_n$ versus μ for each tube in each system, although most authors have presented ΔT as a function of μ. It was hoped that this study would produce evidence in support of, or contradicting, Solokov's (12) theory that $\Delta T/T_n$, rather than ΔT, is constant for given values of μ and $\mathbb{P}$. The input temperature range recorded -- 64°F to 94°F -- would result in a variation of only 5.5 per cent in $\Delta T/T_n$ if ΔT remained constant. This change, unfortunately, was too small for any conclusive evidence to be produced.

The curve shapes in the current data showed great similarity to those recorded by Martynovskii and Alekseev (5) and disagreed substantially with Solokov's theoretical curves: Solokov shows $\Delta T_h/T_n$ increasing from 0 at $\mu=0$ to a maximum at approximately $\mu=0.8$. It then decreases to 0 at a value of μ slightly less than one. (This decrease was seen in one case -- see Figure 11.) Solokov's $\Delta T_c/T_n$ increases continuously with increasing μ, reaching zero at the point $\Delta T_h/T_n$ reaches zero. This disagreement may be due to differences in the positions and methods of temperature and pressure measurements. This author measured temperature merely by placing a thermocouple in the moving stream of air. Pressures at the inlet were

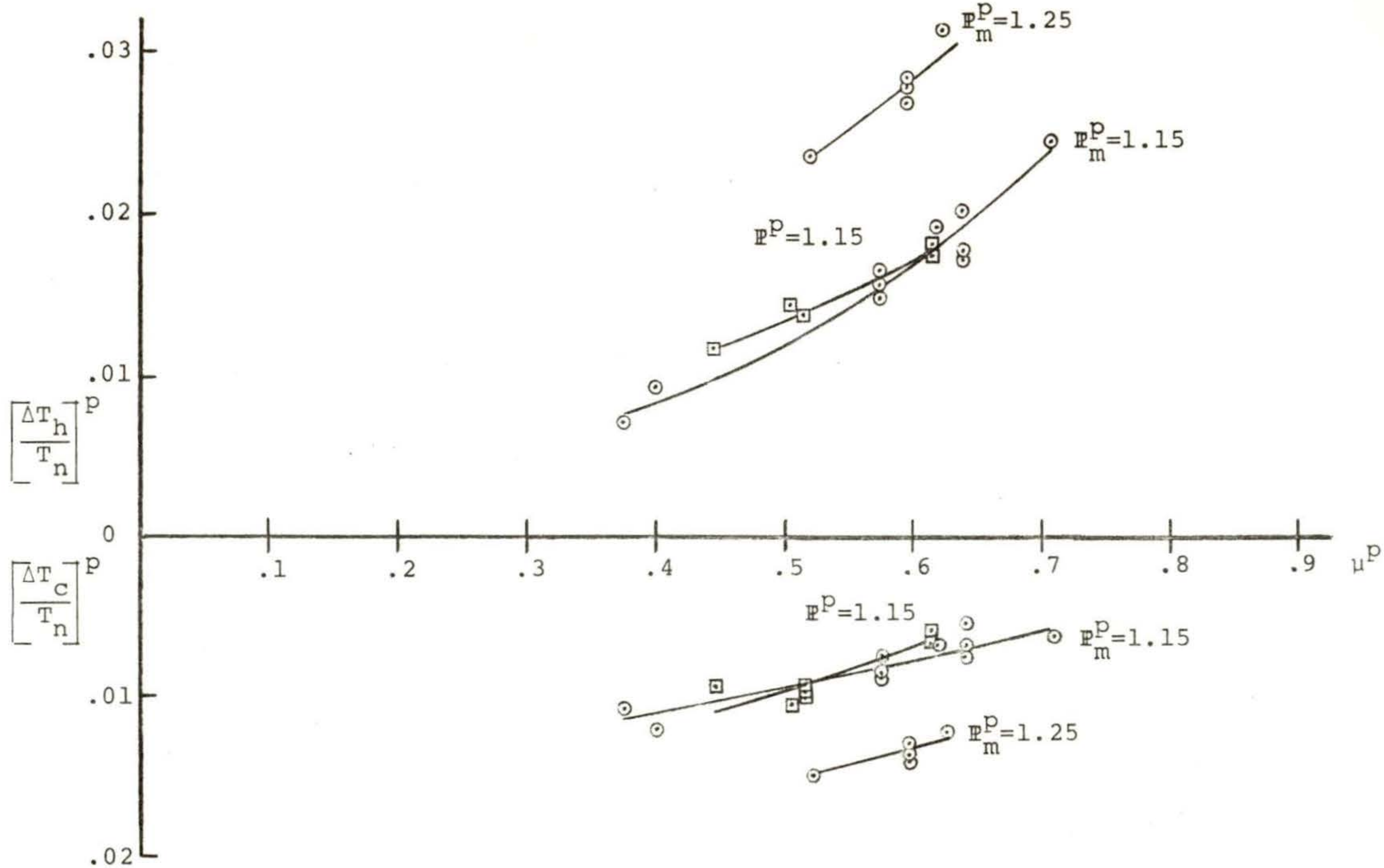

Figure 10. Temperature ratio versus flow ratio. Primary tube, system 2

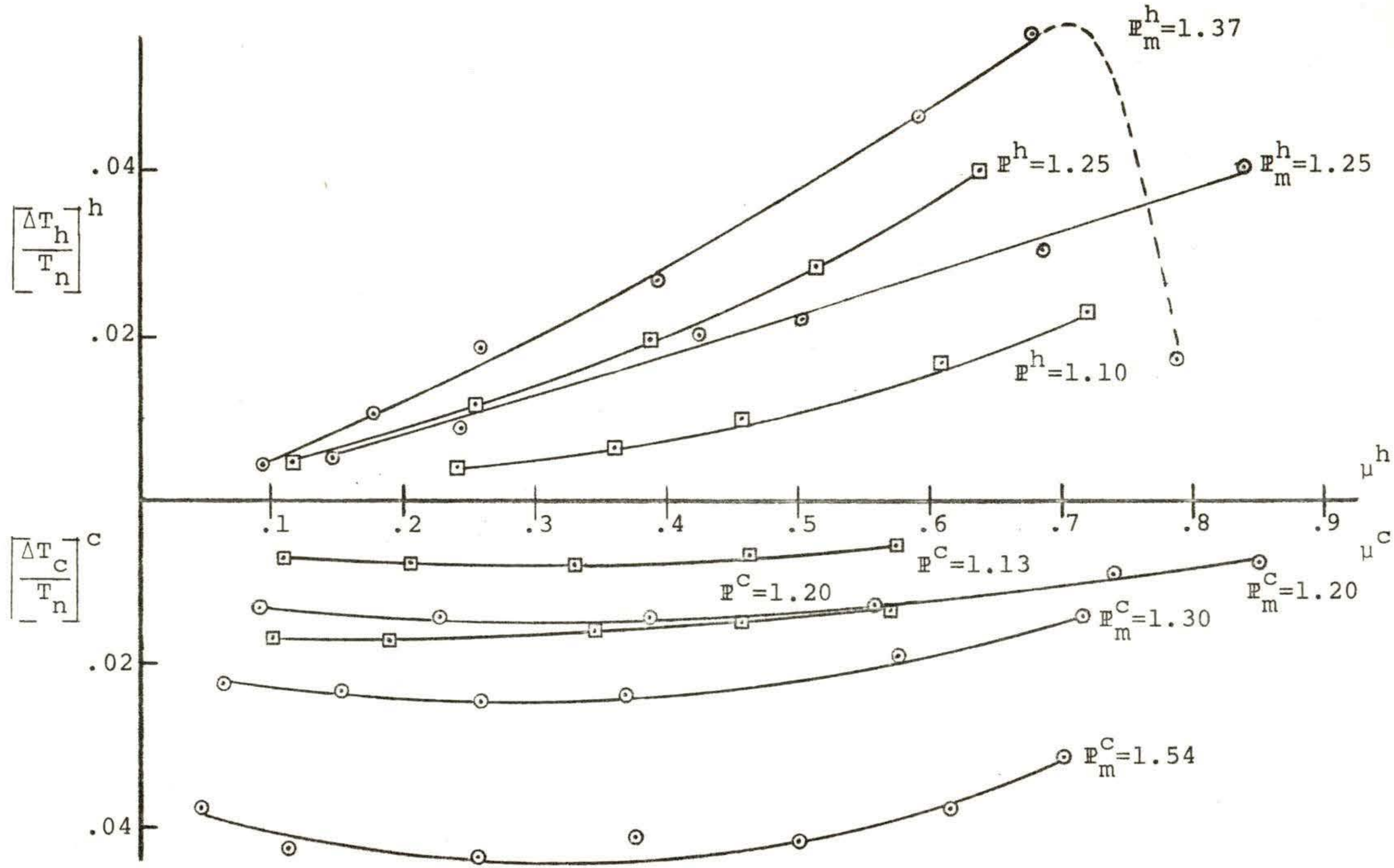

Figure 11. Temperature ratio versus flow ratio. Secondary H and secondary C, system 2

measured before the air entered the inlet channel and measured in the cold stream just beyond the cold orifice.

The author's opinion is that the cascaded vortex tube system does not lend itself well to a similitude study. The parameters involved in obtaining a temperature separation become nebulous when the operation of one tube is dependent upon the output of another. One setting of the primary tube's characteristics, for example, may severely restrict the operation of the secondaries -- the values of $\mathbb{P}^c$ or $\mathbb{P}^h$ are fixed by the settings of the exhaust valves to that secondary (which also govern the operation of the primary). These pressure ratios may be varied only by means of a third valve, controlling the output stream of the primary (the secondary's input), to maintain $\mathbb{P}^p$ and μ^p. This allows the secondary exhaust valves to be opened further to attain a greater pressure ratio. (The head loss across that third valve, however, significantly decreases the pressure available at the input to the secondary.) The interdependence of these pressure ratios and flow rate ratios is affected by the size of the model as well as factors which may be difficult to model accurately (i.e., head loss across a valve or a T-connector).

Predictions concerning the modeling of single vortex tubes were made on the basis of Smith's (11) findings -- that the tubes could be treated as a true model (prediction factor of 1.0 ± 0.004). Current data do not confirm Smith's results,

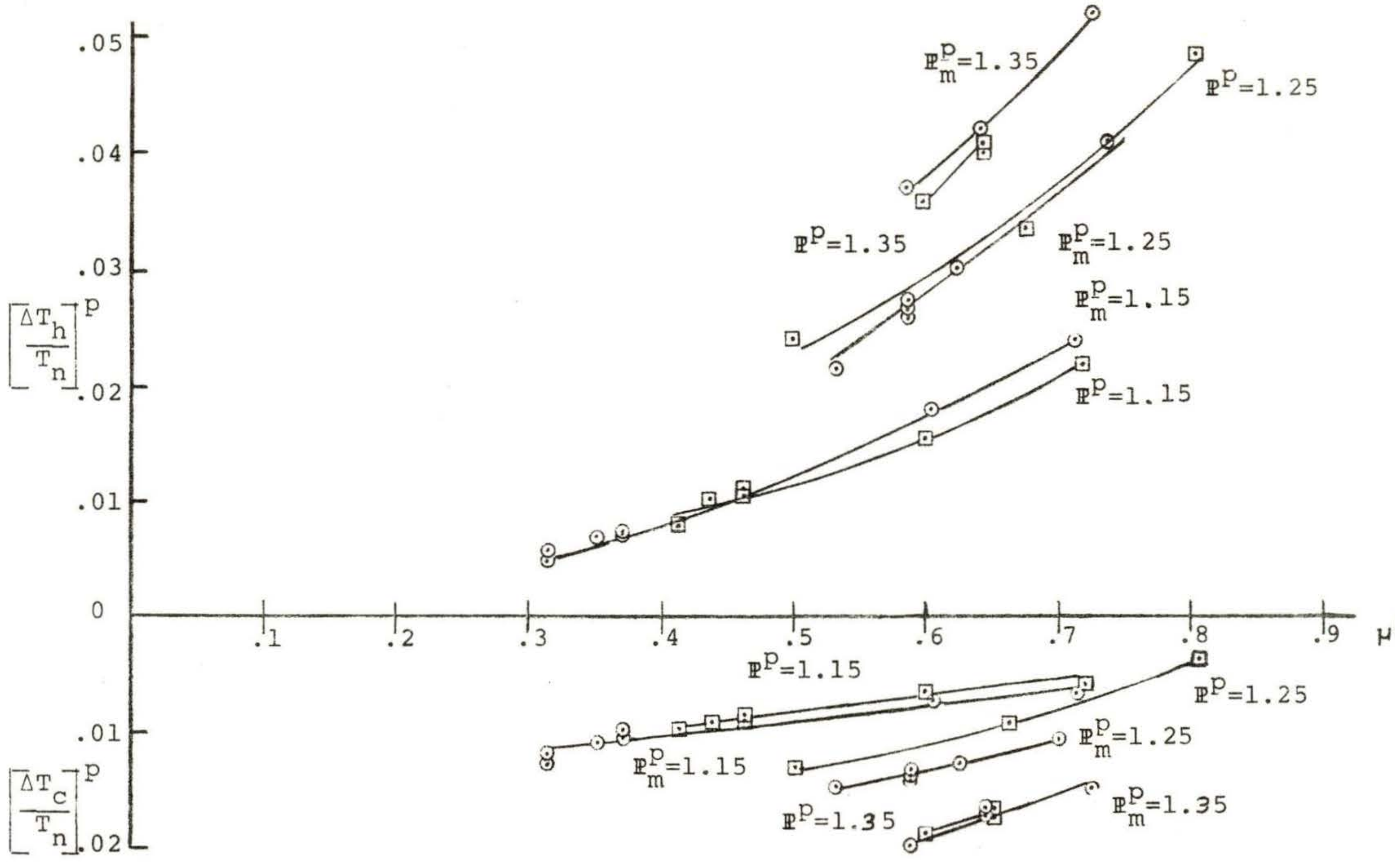

Figure 12. Temperature ratio versus flow ratio. Primary tube, system 3

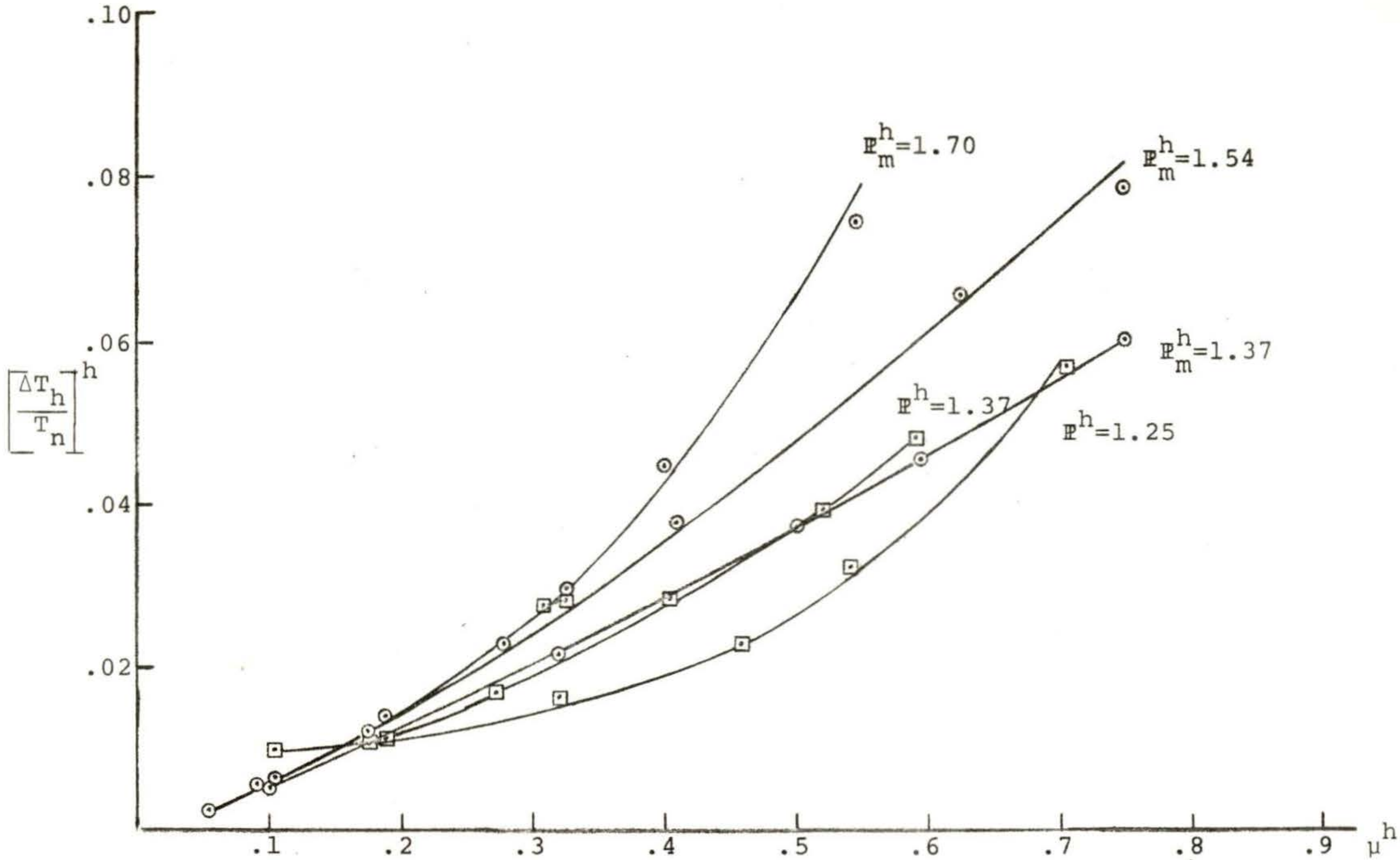

Figure 13. Temperature ratio versus flow ratio. Secondary H, system 3

but shows that the cooling effect was enhanced slightly in larger vortex tubes (as seen also by Martynovskii and Alekseev (5) and Hilsch (3)). The temperature rise curves showed a greater concavity as tube diameter increased, although $\Delta T_h/T_n$ was similar over the central region of the graph. (See Figures 9, 11, and 13.) The data obtained from the primary tubes was not consistent. This inconsistency is probably due to rather large errors seen in the rotameters measuring flows through the primary tube. The accuracy of these devices was stated to be $\pm$ 2% -- resulting in a possible deviation in μ^p of approximately 0.08. In addition the floats were quite unsteady and, except at greater flow rates, tended to oscillate, making accurate measurements difficult to obtain. Pressure corrections were also made, reflecting the inaccuracy of both pressure gauges and the author's reading of the pressure correction curves in the final data. The flow rates through the secondary tubes are believed to be more accurate: These rotameters were designed for greater accuracy, their floats were very stable, and no pressure corrections were made since they exhausted to atmospheric pressure. Data from the secondary tubes were seen to be reproducible while data from the primary were not.

This study obtained results differing from Smith's in another effect. Smith reported no maximum temperature drop, which, according to Martynovskii and Alekseev (5), occurs at approximately μ=0.3. Smith attributed this decrease in ΔT_c

at small μ's to heat conduction from the surroundings through the components of the vortex tube. He said that this effect was minimized by the low thermal conductivity of Plexiglas. (Most previous research had employed copper vortex tubes.) This assumption is refuted by current data, also obtained via Plexiglas vortex tubes. No explanation for this discrepancy occurs to this author.

CONCLUSIONS AND RECOMMENDATIONS

This author's experience with a cascaded system indicated that modeling of such a system might be difficult as a result of the size dependent inter-relationships of various parameters. Operation also depended upon factors not easily modeled, i.e. head losses.

The present study also indicated that the temperature drop and temperature rise occurring in the vortex tube is only slightly dependent upon input temperature, if at all. The range of input temperatures was insufficient to determine the exact dependence upon this factor.

Present data was noted to differ from Smith's in two ways: The prediction equation did not yield a prediction factor of essentially 1.0, but rather is expected to be a function of one or more π-terms. Also, a maximum in ΔT_c was seen at approximately μ=0.3. This maximum was not reported by Smith.

The author recommends additional studies in the following areas:

1. Further research toward the determination of the prediction factor in a similitude study of vortex tubes,
2. application of the cascaded system of vortex tubes to the operation of an electrical generating station (employing the hot stream in a feed-water heater and cooling condenser effluent with the cold stream),
3. determination of optimum conditions for the

operation of the cascaded system of vortex tubes,

4. extension of the range of the pressure ratios and flow rate ratios in the primary vortex tube.

BIBLIOGRAPHY

1. Brodyanskii, V. M. and Martynov, A. V. Dependence of the Ranque-Hilsch Effect on Temperature. Thermal Engineering 11(6): 99-102. 1964.

2. Cooney, D. O. Transient Phenomena Observed during Operation of a Ranque-Hilsch Vortex Tube. Industrial and Engineering Chemistry 10: 308-309. 1971.

3. Hilsch, R. The Use of the Expansion of Gases in a Centifugal Field as a Cooling Process. Review of Scientific Instruments 18: 108-114. 1947.

4. Lay, J. E. An Experimental and Analytical Study of Vortex-Flow Temperature Separation by Superposition of Spiral and Axial Flows. Journal of Heat Transfer Ser. C, 81: 202-222. 1959.

5. Martynovskii, V. S. and Alekseev, V. P. Investigation of the Vortex Thermal Separation Effect for Gases and Vapors. Soviet Physics - Technical Physics 1: 2233-2243. 1956.

6. Merkulov, A. P. Simultaneous Working of a Vortex Tube and a Diffuser (in Russian). Abstracted in Applied Mechanical Reviews 17: 4015. 1964.

7. Merkulov, A. P. and Kolyshev, N. D. An Investigation of the Temperature Fields of a Vortex Tube and a Diffuser (in Russian). Abstracted in Applied Mechanical Reviews 20: 4241. 1967.

8. Murphy, Glenn. Similitude in Engineering. New York, N.Y., The Ronald Press Company. c1950.

9. Scheller, W. A. and Brown, G. M. The Ranque-Hilsch Vortex Tube. Industrial Engineering Chemistry 49: 1013-1018. 1957.

10. Sibulkin, M. Unsteady, Viscous, Circular Flow. Part 3. Application to the Ranque-Hilsch Vortex Tube. Journal of Fluid Mechanics 12: 269-293. 1962.

11. Smith, M. L. Similitude Requirements for Models of a Vortex Tube. Ames, Iowa, Iowa State University. 1966.

12. Solokov, E. Ya. Characteristics of a Vortex Tube. Thermal Engineering 13(7): 84-91. 1966.

13. Starostin, P. I. and Itkin, M. S. Operation of a Vortex Tube on High Pressure Superheated Steam. Thermal Engineering 15(8): 45-51. 1968.

14. Vivian, C. H. The Ranque-Hilsch Tube. Compressed Air Magazine 68(5): 26-28. 1963.

15. Welty, J. R., Wicks, C. E., and Wilson, R. E. Fundamentals of Momentum, Heat, and Mass Transfer. New York, N.Y., John Wiley and Sons, Inc. c1969.

16. Westley, R. A Bibliography and Survey of the Vortex Tube. Cranfield (England) College of Aeronautics Note No. 9. 1954.

ACKNOWLEDGEMENTS

The author wishes to express gratitude to the Department of Nuclear Engineering for the financial support which made his study at Iowa State University possible, and to Dr. Glenn Murphy for his assistance as major professor.

APPENDIX A: DATA

Table 3. System 1 model, data for Figures 8 and 9

Primary tube:

$\mathbb{P}^p_m$	μ^p_m	T^p_{hm}	T^p_{nm}	T^p_{cm}	$\left[\frac{\Delta T_c}{T_n}\right]^p_m$	$\left[\frac{\Delta T_h}{T_n}\right]^p_m$
$\frac{34.7}{30.2} = 1.15$	0.438	81.0	75.2	70.0	0.0097	0.0108
		83.4	77.5	72.5	0.0093	0.0110
		77.5	73.0	67.5	0.0103	0.0085
	0.354	86.0	82.0	75.5	0.0120	0.0074
		76.0	71.3	65.2	0.0115	0.0088
		77.3	72.8	66.4	0.0119	0.0084
	0.500	79.0	72.5	67.5	0.0094	0.0122
		80.0	73.5	68.3	0.0097	0.0122
		80.0	73.5	68.6	0.0091	0.0122
$\frac{44.7}{38.9} = 1.15$	0.512	79.7	73.2	69.5	0.0071	0.0122
		79.8	73.3	69.0	0.0080	0.0122

Secondary H tube:

$\mathbb{P}^h_m$	μ^h_m	T^h_{hm}	T^h_{nm}	$\left[\frac{\Delta T_h}{T_n}\right]^h_m$
$\frac{29.7}{21.7} = 1.37$	0.376	90.0	76.2	0.0258
	0.204	82.0	76.4	0.0104
	0.087	77.4	75.5	0.0036
($\mu^p = 0.438$)	0.500	95.4	76.0	0.0362
	0.670	104.6	76.6	0.0522
	0.745	109.2	76.6	0.0608
$\frac{28.7}{16.9} = 1.70$	0.174	83.6	76.6	0.0131
	0.264	89.5	76.3	0.0246
($\mu^p = 0.354$)	0.372	99.4	76.3	0.0431
	0.595	120.5	77.4	0.0802
	0.735	139.0	77.4	0.1147
	0.083	78.7	76.8	0.0035
	0.490	109.0	76.4	0.0608
$\frac{29.7}{23.7} = 1.25$	0.231	80.1	75.3	0.0090
	0.077	76.6	75.4	0.0022
($\mu^p = 0.500$)	0.346	84.3	75.6	0.0163
	0.514	89.8	76.5	0.0248
	0.720	96.0	76.5	0.0364
	0.410	86.7	76.5	0.0190

Table 3 (Continued)

Secondary C tube:

$\mathbb{E}_m^C$	μ_m^C	T_{nm}^C	T_{cm}^C	$\left[\frac{\Delta T_c}{T_n}\right]_m^C$
$\frac{30.2}{17.7} = 1.70$	0.262	71.5	51.0	0.0386
	0.157	71.0	52.5	0.0349
(μ^P = 0.438)	0.089	71.0	52.8	0.0343
	0.314	74.2	52.8	0.0401
	0.508	74.2	53.5	0.0390
	0.745	73.4	59.8	0.0255
	0.626	73.2	55.0	0.0342
$\frac{30.2}{23.2} = 1.30$	0.402	75.5	65.2	0.0192
	0.286	75.3	65.2	0.0189
(μ^P = 0.354)	0.590	74.0	66.0	0.0150
	0.785	73.8	71.0	0.0052
	0.340	73.0	62.4	0.0190
	0.080	68.0	59.8	0.0155
$\frac{30.2}{15.7} = 1.92$	0.064	68.6	46.8	0.0413
	0.141	68.6	42.8	0.0488
(μ^P = 0.500)	0.270	68.6	40.8	0.0526
	0.430	68.6	41.3	0.0517
	0.590	68.6	46.8	0.0413
	0.668	69.5	50.5	0.0359
$\frac{25.8}{15.2} = 1.70$	0.316	70.0	48.9	0.0398
	0.155	70.0	50.0	0.0378
(μ^P = 0.512)	0.472	70.0	50.5	0.0368

Table 4. System 1 prototype, data for Figures 8 and 9

Primary tube:

$\mathbb{P}^p$	μ^p	T_h^p	T_n^p	T_c^p	$\left[\frac{\Delta T_c}{T_n}\right]^p$	$\left[\frac{\Delta T_h}{T_n}\right]^p$
$\frac{34.7}{30.2} = 1.15$	0.428	82.0	76.3	71.8	0.0084	0.0106
		83.3	77.5	73.0	0.0084	0.0108
		83.4	77.5	72.8	0.0080	0.0110
	0.383	84.5	80.2	74.8	0.0100	0.0080
		84.0	79.7	74.8	0.0091	0.0080
		84.5	80.0	74.8	0.0096	0.0083
	0.464	85.7	79.7	75.0	0.0087	0.0111
		85.0	79.0	74.4	0.0085	0.0111
		85.0	80.0	75.3	0.0087	0.0093

Secondary H tube:

$\mathbb{P}^h$	μ^h	T_h^h	T_n^h	$\left[\frac{\Delta T_n}{T_n}\right]^h$
$\frac{26.2}{19.0} = 1.37$	0.421	97.2	81.4	0.0292
	0.590	107.8	81.4	0.0488
	0.505	102.7	81.4	0.0394
($\mu^p = 0.428$)	0.360	95.0	81.8	0.0244
	0.253	90.0	81.4	0.0159
	0.129	87.6	81.8	0.0107
$\frac{25.7}{17.7} = 1.45$	0.282	96.3	81.8	0.0268
	0.460	103.6	81.8	0.0397
	0.360	99.3	81.8	0.0323
($\mu^p = 0.383$)	0.256	95.3	81.4	0.0257
$\frac{27.2}{21.7} = 1.25$	0.510	98.0	82.2	0.0292
	0.630	107.8	82.2	0.0476
	0.383	93.4	82.2	0.0207
($\mu^p = 0.464$)	0.285	89.7	82.2	0.0138
	0.150	86.3	82.2	0.0076
	0.570	101.4	82.0	0.0358

Table 4 (Continued)

Secondary C tube:

$\mathbb{F}^c$	μ^c	T_n^c	T_c^c	$\left[\frac{\Delta T_c}{T_n}\right]^c$
$\frac{28.2}{16.7} = 1.70$	0.206	76.6	53.0	0.0440
	0.098	77.0	55.0	0.0410
	0.338	77.4	53.7	0.0441
$(\mu^p = 0.428)$	0.414	77.4	54.8	0.0421
	0.525	77.4	56.0	0.0398
	0.600	77.4	57.3	0.0374
$\frac{28.7}{19.7} = 1.45$	0.435	77.4	61.8	0.0290
	0.536	77.8	63.2	0.0272
	0.710	77.8	68.0	0.0171
$(\mu^p = 0.383$	0.248	78.0	62.0	0.0298
	0.330	78.0	61.4	0.0309
	0.178	78.0	63.2	0.0275
$\frac{28.7}{15.7} = 1.83$	0.208	79.5	53.2	0.0488
	0.138	77.4	52.0	0.0473
	0.298	77.4	51.0	0.0492
	0.350	79.5	54.0	0.0473

Table 5. System 2 model, data for Figures 10 and 11

Primary tube:

$\mathbb{P}_m^p$	μ_m^p	T_{hm}^p	T_{nm}^p	T_{cm}^p	$\left[\frac{\Delta T_c}{T_n}\right]_m^p$	$\left[\frac{\Delta T_h}{T_n}\right]_m^p$
$\frac{34.7}{30.2} = 1.15$	0.574	85.0	76.1	72.1	0.0075	0.0166
		84.1	76.1	71.5	0.0086	0.0149
		84.5	76.1	71.4	0.0088	0.0157
	0.620	85.4	75.2	71.5	0.0069	0.0191
	0.708	87.4	74.4	71.0	0.0064	0.0243
	0.400	80.0	75.0	68.6	0.0120	0.0094
	0.375	79.2	75.4	69.7	0.0107	0.0071
	0.640	86.3	75.5	71.5	0.0075	0.0202
		84.7	75.5	72.6	0.0054	0.0172
		85.0	75.6	71.9	0.0069	0.0176
$\frac{34.7}{27.7} = 1.25$	0.596	88.7	73.9	66.6	0.0137	0.0277
		90.4	76.1	68.6	0.0140	0.0267
		90.6	75.5	68.6	0.0129	0.0282
	0.622	92.2	75.5	69.0	0.0121	0.0312
	0.520	88.0	75.5	67.0	0.0159	0.0234

Secondary H tube:

$\mathbb{P}_m^h$	μ_m^h	T_{hm}^h	T_{nm}^h	$\left[\frac{\Delta T_h}{T_n}\right]_m^h$
$\frac{29.7}{23.7} = 1.25$	0.426	88.4	77.4	0.0205
	0.685	95.5	78.0	0.0325
	0.505	91.1	78.0	0.0246
($\mu^p = 0.574$)	0.840	99.7	78.0	0.0404
	0.244	83.0	78.0	0.0093
	0.145	81.4	78.5	0.0054
$\frac{27.7}{20.2} = 1.37$	0.259	89.5	80.8	0.0186
	0.093	83.2	80.8	0.0044
($\mu^p = 0.596$)	0.179	86.3	80.5	0.0107
	0.395	95.5	80.8	0.0272
	0.594	105.7	80.8	0.0461
	0.680	112.5	82.0	0.0563
	0.790	91.5	82.0	0.0175

Table 5. System 2 model, data for Figures 10 and 11

Primary tube:

E_m^p	μ_m^p	$T_{\ell m}^p$	T_{nm}^p	T_{cm}^p	$\left[\frac{\Delta T_c}{T_n}\right]_m^p$	$\left[\frac{\Delta T_n}{T_n}\right]_m^p$
$\frac{34.7}{30.2} = 1.15$	0.574	85.0	76.1	72.1	0.0075	0.0166
		84.1	76.1	71.5	0.0086	0.0149
		84.5	76.1	71.4	0.0088	0.0157
	0.620	85.4	75.2	71.5	0.0069	0.0191
	0.708	87.4	74.4	71.0	0.0064	0.0243
	0.400	80.0	75.0	68.6	0.0120	0.0094
	0.375	79.2	75.4	69.7	0.0107	0.0071
	0.640	86.3	75.5	71.5	0.0075	0.0202
		84.7	75.5	72.6	0.0054	0.0172
		85.0	75.6	71.9	0.0069	0.0176
$\frac{34.7}{27.7} = 1.25$	0.596	88.7	73.9	66.6	0.0137	0.0277
		90.4	76.1	68.6	0.0140	0.0267
		90.6	75.5	68.6	0.0129	0.0282
	0.622	92.2	75.5	69.0	0.0121	0.0312
	0.520	88.0	75.5	67.0	0.0129	0.0234

Secondary II tube:

E_m^n	μ_m^n	$T_{\ell m}^n$	T_{nm}^n	$\left[\frac{\Delta T_n}{T_n}\right]_m^n$
$\frac{29.7}{23.7} = 1.25$	0.426	88.4	77.4	0.0202
	0.683	95.5	78.0	0.0325
	0.505	91.1	78.0	0.0246
($\mu^p = 0.574$)	0.840	99.7	78.0	0.0404
	0.244	83.0	78.0	0.0093
	0.145	81.4	78.5	0.0054
$\frac{27.7}{20.2} = 1.37$	0.259	89.5	80.8	0.0186
	0.093	83.2	80.8	0.0044
($\mu^p = 0.596$)	0.179	86.3	80.5	0.0107
	0.395	95.5	80.8	0.0272
	0.594	105.7	80.8	0.0461
	0.680	112.5	82.0	0.0563
	0.790	91.5	82.0	0.0175

Table 5 (Continued)

Secondary C tube:

$\mathbb{P}^{c}$	μ^{c}	T_n^{c}	T_c^{c}	$\left[\frac{\Delta T_c}{T_n}\right]^{c}$
$\frac{30.2}{25.2} = 1.20$	0.558	75.3	68.5	0.0127
	0.740	75.0	70.0	0.0094
$(\mu^{p} = 0.574)$	0.850	75.0	71.0	0.0075
	0.386	75.3	67.7	0.0142
	0.228	75.0	67.5	0.0140
	0.091	75.0	68.1	0.0129
$\frac{26.2}{17.0} = 1.54$	0.113	75.0	52.3	0.0425
	0.046	75.0	55.0	0.0374
$(\mu^{p} = 0.596)$	0.256	75.0	51.8	0.0434
	0.375	75.0	52.3	0.0408
	0.500	75.0	52.8	0.0415
	0.616	75.0	55.0	0.0374
	0.700	75.0	58.3	0.0312
$\frac{30.2}{23.2} = 1.30$	0.574	74.1	64.0	0.0190
	0.716	74.5	67.0	0.0141
$(\mu^{p} = 0.640)$	0.369	74.5	61.8	0.0238
	0.258	74.5	61.5	0.0243
	0.153	74.5	62.0	0.0234
	0.062	74.8	62.8	0.0225

Table 6. System 2 prototype, data for Figures 10 and 11

Primary tube:

$\mathbb{P}^p$	μ^p	T_n^p	T_n^p	T_c^p	$\left[\frac{\Delta T_c}{T_n}\right]^p$	$\left[\frac{\Delta T_h}{T_n}\right]^p$
$\frac{34.7}{30.2} = 1.15$	0.615	95.0	84.5	81.3	0.0059	0.0175
		92.8	83.0	79.3	0.0068	0.0181
		92.0	82.2	79.0	0.0059	0.0181
	0.515	91.5	84.0	79.0	0.0092	0.0138
		91.5	84.0	78.8	0.0096	0.0138
		91.5	84.0	78.6	0.0100	0.0138
	0.445	88.4	82.0	77.0	0.0093	0.0118
	0.505	89.7	83.0	77.3	0.0105	0.0125

Secondary H tube:

$\mathbb{P}^h$	μ^h	T_h^h	T_n^h	$\left[\frac{\Delta T_h}{T_n}\right]^h$
$\frac{28.7}{26.2} = 1.10$	0.610	97.7	88.4	0.0170
	0.457	94.0	88.4	0.0102
	0.233	90.8	88.4	0.0044
(μ^p = 0.615)	0.360	92.0	88.4	0.0066
	0.720	101.0	88.4	0.0230
$\frac{26.7}{21.4} = 1.25$	0.515	102.8	87.3	0.0284
	0.636	109.0	87.3	0.0398
	0.388	98.8	88.0	0.0197
(μ^p = 0.515)	0.255	94.5	88.0	0.0119
	0.115	90.6	88.0	0.0048

Secondary C tube:

$\mathbb{P}^c$	μ_c	T_n^c	T_n^c	$\left[\frac{\Delta T_c}{T_n}\right]^c$
$\frac{23.7}{19.7} = 1.20$	0.570	82.5	75.5	0.0129
	0.346	79.5	71.0	0.0158
	0.192	83.0	74.0	0.0167
	0.100	79.5	70.8	0.0161
	0.457	79.8	72.1	0.0145
$\frac{25.7}{22.7} = 1.13$	0.464	78.3	75.0	0.0062
	0.573	78.3	75.3	0.0056
	0.330	78.3	74.1	0.0078
	0.205	78.3	74.2	0.0076
	0.108	78.3	74.5	0.0071

Table 7. System 3 model, data for Figures 12 and 13

Primary tube:

$\mathbb{P}_m^p$	μ_m^p	T_{hm}^p	T_{nm}^p	T_{cm}^p	$\left[\frac{\Delta T_c}{T_n}\right]_m^p$	$\left[\frac{\Delta T_h}{T_n}\right]_m^p$
$\frac{34.7}{30.2} = 1.15$	0.372	68.5	64.5	59.0	0.0105	0.0076
		68.0	64.1	59.0	0.0097	0.0074
		68.0	64.0	58.5	0.0105	0.0076
	0.352	67.7	64.0	58.4	0.0107	0.0071
	0.314	66.5	64.0	57.8	0.0118	0.0048
		79.5	76.2	69.5	0.0125	0.0061
	0.606	86.3	76.6	72.7	0.0073	0.0181
	0.714	89.5	76.6	73.0	0.0067	0.0241
$\frac{34.7}{25.7} = 1.35$	0.645	88.4	66.3	57.8	0.0162	0.0420
		91.0	68.8	59.8	0.0170	0.0420
	0.728	97.2	68.8	61.0	0.0148	0.0537
$\frac{44.7}{33.2} = 1.35$	0.589	89.7	70.0	59.6	0.0196	0.0372
$\frac{34.7}{27.7} = 1.25$	0.585	87.3	73.0	65.5	0.0141	0.0268
		87.7	73.0	65.7	0.0137	0.0276
		86.9	73.0	66.0	0.0131	0.0261
	0.625	90.0	73.0	66.3	0.0126	0.0319
	0.740	95.0	73.0	67.4	0.0105	0.0413
	0.532	84.5	73.0	65.3	0.0145	0.0216

Secondary H tube:

$\mathbb{P}_m^h$	μ_m^h	T_{hm}^h	T_{nm}^h	$\left[\frac{\Delta T_h}{T_n}\right]_m^h$
$\frac{29.2}{17.2} = 1.70$	0.104	70.0	66.6	0.0065
	0.054	68.0	66.8	0.0023
($\mu^p = 0.372$)	0.173	72.8	66.4	0.0122
	0.327	82.0	66.3	0.0298
	0.545	105.8	66.6	0.0745
	0.400	90.7	67.0	0.0450
$\frac{25.7}{16.7} = 1.54$	0.750	126.0	83.2	0.0788
	0.625	119.0	83.2	0.0659
($\mu^p = 0.645$)	0.410	103.6	83.0	0.0380
	0.280	95.6	83.0	0.0232
	0.187	90.5	83.0	0.0138
	0.093	86.2	83.0	0.0059

Table 7 (Continued)

Secondary H tube: (Continued)

$\mathbb{P}_m^h$	μ_m^h	T_{hm}^h	T_{nm}^h	$\left[\frac{\Delta T_h}{T_n}\right]_m^h$
$\frac{27.2}{19.7} = 1.37$	0.750	113.4	80.8	0.0603
	0.500	101.4	81.0	0.0377
($\mu^p = 0.585$)	0.595	105.8	81.0	0.0459
	0.320	92.8	81.0	0.0218
	0.100	84.7	81.8	0.0054

Table 8. System 3 prototype, data for Figures 12 and 13

Primary tube:

$\mathbb{P}^p$	μ^p	T_n^p	T_n^p	T_c^p	$\left[\frac{\Delta T_c}{T_n}\right]^p$	$\left[\frac{\Delta T_h}{T_n}\right]^p$
$\frac{34.7}{30.2} = 1.15$	0.462	85.4	79.7	75.0	0.0087	0.0106
		85.8	80.0	75.3	0.0087	0.0107
		85.7	79.7	75.2	0.0083	0.0111
	0.436	85.3	79.7	75.0	0.0087	0.0104
	0.415	84.5	80.2	75.0	0.0096	0.0080
	0.600	88.5	80.0	76.5	0.0065	0.0157
	0.720	92.4	80.5	77.4	0.0057	0.0220
$\frac{34.7}{27.7} = 1.25$	0.500	94.6	81.4	74.5	0.0128	0.0244
		94.2	81.0	77.0	0.0129	0.0244
	0.678	99.3	81.0	76.3	0.0087	0.0338
	0.805	107.8	81.5	79.7	0.0033	0.0486
$\frac{34.7}{25.7} = 1.35$	0.645	106.6	84.5	75.3	0.0169	0.0409
		106.6	84.8	75.7	0.0167	0.0401
		106.3	84.8	75.5	0.0171	0.0396
	0.600	103.6	84.0	74.2	0.0180	0.0361

Secondary H tube:

$\mathbb{P}^h$	μ^h	T_h^h	T_n^h	$\left[\frac{\Delta T_h}{T_n}\right]^h$
$\frac{26.2}{19.2} = 1.37$	0.520	103.6	82.2	0.0395
	0.593	108.5	82.2	0.0485
	0.405	98.6	83.0	0.0287
($\mu^p = 0.462$)	0.272	92.0	83.0	0.0166
	0.188	89.3	83.0	0.0116
	0.104	87.8	82.2	0.0103
$\frac{23.7}{16.4} = 1.45$	0.308	104.0	88.8	0.0277
	0.324	104.0	88.5	0.0283
($\mu^p = 0.500$)				
$\frac{23.7}{19.0} = 1.25$	0.458	107.8	94.0	0.0249
	0.705	126.8	95.0	0.0573
	0.540	114.0	96.0	0.0324
	0.320	104.2	95.0	0.0166
	0.176	100.6	94.5	0.0110

APPENDIX B: APPARATUS

The apparatus consisted of six vortex tubes, the necessary Tygon tubing, connectors, and valves to create a cascaded system, and the accompanying pressure, temperature, and flow rate metering equipment.

The pressure was measured by means of six dial-type pressure gauges, one capable of measuring to 100 psig, one measuring to 60 psig, one to 30 psig, and three to 15 psig. All were obtained through Central Stores and were manufactured by Marshalltown Gauge, Marsh Instrument Company, and Weksler Instruments.

Two rotameters had a rated capacity of 26 SCFM and were obtained from Fischer-Porter Company, Warminster, Pennsylvania. Two had capacities of 10.5 and 2.2 SCFM and were ordered from Wallace & Tiernan Division, Penwalt Corporation, Belleville, New Jersey. All capacities are given at 14.7 psi and 70°F. The smaller flow meters were used at these conditions, but pressure correction curves were used with the two 26 SCFM rotameters. All rotameters claimed an accuracy of 2 per cent of rated capacity.

The temperature was measured by means of copper-constantan thermocouples. The potential supplied by these thermocouples was measured on a potentiometer manufactured by Rubicon Instruments, a division of Honeywell, Philadelphia, Pennsylvania.